Variation of geometries and electron properties along proton transfer in strong hydrogen-bond complexes

ARTICLE *in* THE JOURNAL OF CHEMICAL PHYSICS · JULY 2005

Impact Factor: 2.95 · DOI: 10.1063/1.1899103 · Source: PubMed

3 AUTHORS:

Luis F Pacios
Universidad Politécnica de Madrid
103 PUBLICATIONS **2,097** CITATIONS
SEE PROFILE

Oscar Gálvez
Spanish National Research Council
68 PUBLICATIONS **713** CITATIONS
SEE PROFILE

Pedro C Gómez
Complutense University of Madrid
50 PUBLICATIONS **570** CITATIONS
SEE PROFILE

Variation of geometries and electron properties along proton transfer in strong hydrogen-bond complexes

L. F. Pacios[a)]
Unidad de Química, Departamento de Biotecnología, E.T.S.I. Montes, Universidad Politécnica de Madrid, Madrid 28040, Spain

O. Gálvez[b)] and P. C. Gómez[c)]
Departamento de Química Física I, Facultad de Química, Universidad Complutense de Madrid, Madrid 28040, Spain

(Received 8 February 2005; accepted 9 March 2005; published online 3 June 2005)

Proton transfer in hydrogen-bond systems formed by 4-methylimidazole in both neutral and protonated cationic forms and by acetate anion are studied by means of MP2/6-311++G(d,p) *ab initio* calculations. These two complexes model the histidine (neutral and protonated)-aspartate diad present in the active sites of enzymes the catalytic mechanism of which involves the formation of strong hydrogen bonds. We investigate the evolution of geometries, natural bond orbital populations of bonds and electron lone pairs, topological descriptors of the electron density, and spatial distributions of the electron localization function along the process N-H···O $\rightarrow$N···H···O$\rightarrow$N···H-O, which represents the stages of the H-transfer. Except for a sudden change in the population of electron lone pairs in N and O at the middle N···H···O stage, all the properties analyzed show a smooth continuous behavior along the covalent $\rightarrow$ hydrogen bond transit inherent to the transfer, without any discontinuity that could identify a formation or breaking of the hydrogen bond. This way, the distinction between covalent or hydrogen-bonding features is associated to subtle electron rearrangement at the intermolecular space. © *2005 American Institute of Physics*. [DOI: 10.1063/1.1899103]

I. INTRODUCTION

If one considers the intense research activity in recent years on hydrogen bonding, not only on systems showing disparate binding energies but also on fundamental aspects of its associated features, it is surprising that the physical nature of the interaction is still a matter of debate.[1–10] After more than eight decades of studies the issue whether hydrogen bonding can be described in purely electrostatic terms or whether covalent effects are necessary to understand the interaction is still under discussion. The electronic nature of hydrogen bonding was the subject of controversy from the very first studies, as illustrated by the opposite views of Lewis, who attributed the bonding to a "secondary valence" of hydrogen,[1] and Pauling, who argued that bonding forces are ionic in nature and proposed the conventional electrostatic picture.[2] Although most researchers adhered to this last view until a decade or so, an increasing number of reports published in recent years on hydrogen bonding have defied the electrostatic image. A number of experimental observations supplied by NMR[11–14] and IR[15–17] spectroscopies, x-ray Compton scattering measurements,[18,19] and structural characteristics[20–23] cannot be explained by purely electrostatic models. In this regard, it is illustrative that recent studies on the geometrical features of hydrogen bonds between amino acid side chains in a large data set of high-resolution protein-crystal structures[22,23] led not only to the conclusion that the electrostatic model "ignores some of the essential physical chemistry"[22] but also to the statement: "Hydrogen bonds are partially covalent interactions…."[23] On the theoretical side, it is hard to see how purely electrostatic descriptions could account for the plethora of results spanning so wide a range of interaction strengths and features,[24–32] from weak unconventional[27–29] to short strong hydrogen bonds.[30–32] The discussions about the physical nature of hydrogen bonding, arising from the theoretical evidence accumulated over the last years, have been reviewed elsewhere. The reader may find representative accounts of the subject in the introductions of Refs. 4, 6, 7, and 32.

If few theoretical chemists would disagree with the suggestion that performing quantum calculations is the proper way to treat hydrogen-bonding systems, one should wonder why the ultimate nature of the interaction can still be a matter of debate. No doubt the answer is related with the fact that hydrogen-bonding features are somewhat midway between those of strong covalent bonding and weak van der Waals interactions. Although the results of quantum calculations give molecular orbitals or electron-density distributions, with which one can compute other related functions as well as a variety of numerical descriptors, hydrogen bonding is not easy to characterize in terms of information directly provided by these theoretical objects. As far as the experience in using them has been mostly obtained from covalent bonding, it is obvious that a different viewpoint is needed to

[a)]Author to whom correspondence should be addressed. Electronic mail: lpacios@montes.upm.es
[b)]Electronic mail: ogalvez@quim.ucm.es
[c)]Electronic mail: pgomez@quim.ucm.es

analyze the intermolecular characteristics appearing when a hydrogen bond forms. A comparison of these characteristics with those of well-known covalent bonds seems thus a reasonable avenue to reach a deep understanding of the quantum aspects of hydrogen bonding. In this regard, the atoms in molecules (AIM) methodology developed by Bader[33] and Popelier[34] around the electron density or equivalent analyses proposed by Silvi and Savin and co-workers[35–37] with the electron localization function (ELF) of Becke and Edgecombe[38] constitute invaluable theoretical tools (see Ref. 32 for an illustrative example of the use of both approaches to study hydrogen-bond systems).

We address in this work the quantum characteristics of hydrogen bonding obtained from an *ab initio* study of proton transfer between the partners of two complexes: (i) 4-methylimidazole and acetate anion and (ii) 4-methylimidazolium cation and acetate. These complexes were chosen because they are not only representative examples of strong hydrogen bonding involving charged species but they are also benchmark systems to study at the quantum-level proton transfer between molecular groups like those appearing in reactions catalyzed by enzymes. These complexes represent the side chains of histidine, either unprotonated in (i) or protonated in (ii), and aspartate amino acid residues that form with one nearby serine residue the catalytic triad in active sites of serine proteases and related enzymes.[39–43] Although, obviously, gas-phase isolated complexes cannot be taken as any kind of model for enzymatic processes, our goal in choosing them is twofold. On one side, we aim to explore essential features of the interactions underlying strong hydrogen bonding and how they change with proton transfer occurring through the hydrogen bond. On the other side, we aim further to set a simple reference system to compare experimental observations or theoretical results obtained for realistic models of enzymatic processes in which protons are transferred through hydrogen bonds, a recurrent process occurring in many reactions catalyzed by enzymes.[41] As detailed below, while complex (i) should represent the bare hydrogen-bonding interaction between histidine and asparte in free enzymes where the imidazole ring is unprotonated, complex (ii) should represent the interaction after protonating imidazole, which takes place in enzyme-substrate complexes upon proton donation from nearby residues or water molecules depending on the particular mechanism studied. In this regard, we have shown very recently that these same complexes happen to provide valuable information to rationalize the changes of NMR-proton chemical shifts accompanying H transfer, measured and computed in theoretical realistic models available in the literature.[44]

We have started a research program[6,32,44–47] intended to investigate changes with the intermolecular distance of electron and structural properties of hydrogen-bonding systems (other authors[8] have also added report results in agreement with our findings). By studying H bonds at distances inside and outside of the equilibrium and exploring spatial changes of relevant properties, we aim to complement the picture obtained in the last few years mostly from systems at equilibrium geometry and contribute thus in elucidating essential features of the interaction. The work presented here addresses a different, though related, problem; that is, it investigates changes of these properties when the H atom is transferred from the donor to the acceptor within a complex. This process allows focusing on the transition from covalent to hydrogen bonding to explore which characteristics of the interaction are invariant and which ones are modified in the course of that transition. Alongside the information given by the electron density and the ELF considered before,[6,32,46] we also include electron populations obtained from the natural population analysis (NPA)[48–50] that, as shown below, provides a sensitive probe to trace out those changes.

II. METHODS

The systems studied are depicted in scheme 1 1along with the atom numbering used throughout the paper. They are (i) the anionic complex of 4-methylimidazole and acetate anion, hereafter denoted as Im-Ac(−), and (ii) the neutral

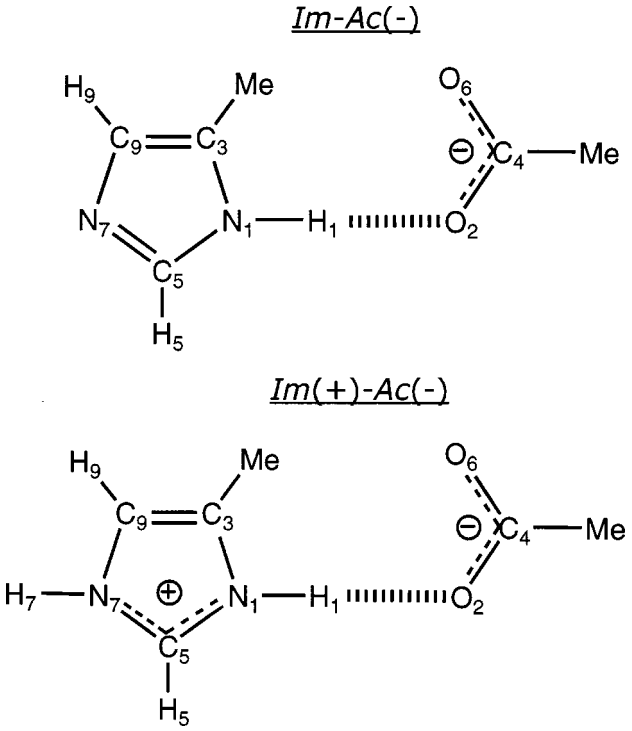

SCHEME 1.

complex of 4-methylimidazolium cation and acetate, denoted as Im(+)-Ac(−). As remarked above, these systems show the interacting groups present in the diad formed by histidine and aspartate side chains that plays a crucial role in the mechanisms of peptide hydrolysis. While, in free enzymes, the diad should be represented by Im-Ac(−), binding the substrate during the catalytic activity occurs upon protonation of imidazole by a nearby residue (usually serine), which should be represented by Im(+)-Ac(−). We stress that these complexes do not intend to mimic actual active sites of enzymes, but in studying them by means of quantum calculations we aim to explore the characteristics of the interaction associated. However, as far as proton transfer along hydrogen bonds from either the neutral (imidazole) or positive

(imidazolium) H donors toward the negative H acceptors (carboxylate) is a ubiquitous process in enzyme mechanisms, this study could also set reference features of potential biochemical interest.

MP2/6-311++G(d,p) *ab initio* calculations were performed to obtain geometries, energies, and electron densities. The treatment of electron-correlation effects underlying hydrogen bonding makes correlated calculations absolutely mandatory, especially to account for intermediate bonding situations linked to the partial stages of proton transfer. Considering the size of the systems and the computational burden in optimizing 26 geometries and performing additional calculations each (see below), we chose MP2 as an affordable yet reliable method to include correlation. The basis set selected is known to achieve a satisfactory compromise between manageable size and flexibility as its ability to yield accurate geometries and energies on hydrogen-bond systems has been demonstrated in recent reports.[6,46,51] Optimized MP2/6-311++G(d,p) geometries were obtained as follows. Isolated Im, Im(+) and Ac(−) monomers were first optimized without constraints and then reoptimized fixing C_{3v} symmetry in methyls which happened to yield negligible differences. Hence we froze C_{3v} internal geometries of methyl groups, although torsion angles with imidazole and carboxylate were optimized in all cases. With this unique constraint, an equilibrium structure with a $N_1\cdots O_2$ intermolecular distance of 2.647 Å and a N_1-H_1 bond length of 1.069 Å was found for Im-Ac(−), whereas optimization predicts for Im(+)-Ac(−) a complete proton transfer resulting in the complex of 4-methylimidazole (with H_7 bonded to N_7) and acetic acid with a $N_1\cdots O_2$ intermolecular distance of 2.751 Å and a H_1-O_2 bond length of 0.998 Å ($N_1\cdots H_1$ distance =1.763 Å). Two sets of optimized geometries were then generated from these equilibrium structures varying the distance between N_1 and H_1 atoms (hereafter denoted R_{NH}) to scan proton transfer through stages N_1-$H_1\cdots O_2$ to $N_1\cdots H_1\cdots O_2$ to $N_1\cdots H_1$-O_2 at a fixed $N_1\cdots O_2$ separation of 2.65 Å for Im-Ac(−) and 2.75 Å for Im(+)-Ac(−). The criterion to set step sizes in these scans was to trace out properly the energy profiles of H transfer which resulted in 11 geometries from R_{NH}=1.00 to 1.70 Å for Im-Ac(−) and 15 geometries from R_{NH}=1.02 to 1.83 Å for Im(+)-Ac(−), yielding energies indicated by dots in Fig. 1. Electron densities were then obtained in separate MP2/6-311++G(d,p) single-point calculations at every geometry, and their critical points were located and characterized according to the AIM theory[33,34] with the program EXTREME.[52] Further calculations were performed to determine electron populations of bonds and lone pairs using the natural population analysis (NPA)[48–50] on natural orbitals obtained at the same level of theory with the program NBO 4.0[53] implemented in the Q-CHEM 2.1[54] package. Geometries and electron densities were obtained with GAUSSIAN 03.[55] Grids to render isocontour maps of electron density and ELF were computed with CHECKDEN[56] from the GAUSSIAN output.

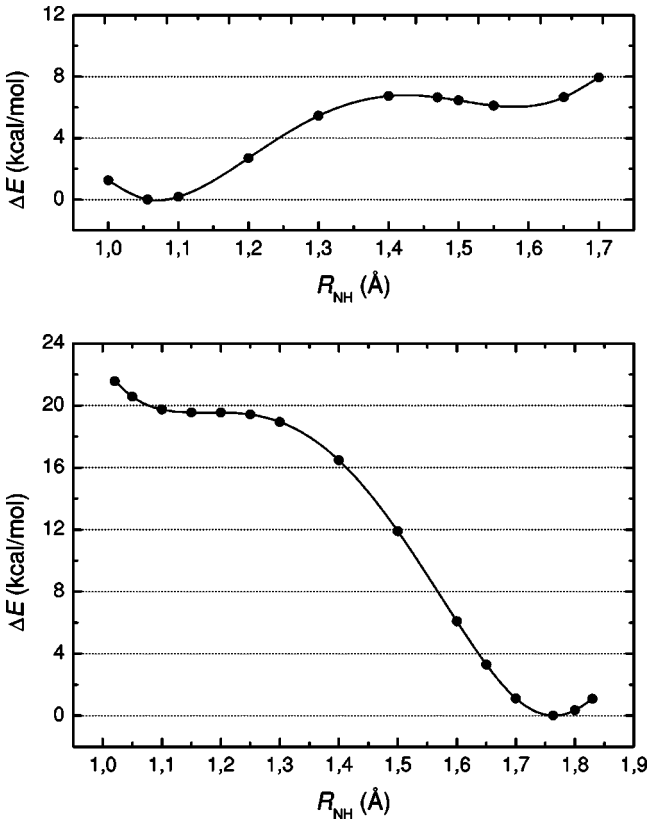

FIG. 1. MP2/6−311++G(d,p) energy profiles for proton transfer in Im-Ac(−) at intermolecular $N_1\cdots O_2$ distance of 2.65 Å (top) and Im(+)-Ac(−) at 2.75 Å (bottom).

III. RESULTS AND DISCUSSION

A. Energy profiles

Profiles in Fig. 1 are determined as energy differences with respect to equilibrium values without inclusion of corrections for basis set superposition error (BSSE). As far as we are interested in information obtained from molecular orbitals and electron densities at distinct stages of the H-transfer process, these corrections are not relevant here. We have studied the energetic issues in these complexes, reporting corrected energies and how they vary under environments of distinct polarity as well as zero-point energy (ZPE) values for equilibrium structures in a separate paper.[57] As noticed in Fig. 1, only the anionic Im-Ac(−) complex exhibits a very low barrier with a height of 6.5 kcal/mol and a second well 6.1 kcal/mol above equilibrium for H transferred to acetate. An uncorrected energy of 30.8 kcal/mol is found for dissociation into Im (with H_1 bonded to N_1) and Ac(−), this value decreasing to 27.1 kcal/mol after correcting for BSSE and 26.2 kcal/mol upon further inclusion of ZPE.[57] The neutral Im(+)-Ac(−) complex behaves rather differently due to the charged nature of its partners. Starting at the left side of the bottom curve in Fig. 1, the energy profile shows a small plateau in the interval $R_{NH}\sim 1.1-1.3$ Å and goes afterward downhill to the minimum at 1.76 Å, where the proton has been transferred to yield neutral acetic acid (H_1 bonded to O_2) and the remaining Im monomer with H_7 is bonded to N_7. Although no barrier is seen in this single-well curve, the plateau height (~19.5 kcal/mol) may be taken as

a rough estimate of the energy gained from the H transfer. However, the dissociation energy depends now on the channel assumed: if one considers dissociation into charged Im(+) and Ac(−) from the minimum, a great energy of 132 kcal/mol is found,[57] which illustrates the strong electrostatic attraction between opposite charges at the intermolecular separation involved. If dissociation into neutral Im (with N_7H_7 bond) and acetic acid is instead considered, an energy one order of magnitude smaller (12 kcal/mol) is obtained,[57] placing the complex in the conventional range of hydrogen-bonding strength which indeed lacks interest for enzymatic processes as neutral acidic groups in proteins are unusual in live systems. In summary the, H transfer from unprotonated imidazole to acetate is a near barrierless process with low energetic cost, whereas protonation of the ring favors the transfer especially after hydrogen moves outside from nitrogen ($R_{NH} \sim 1.3$ Å). As it happens, this H transfer is avoided in actual enzymatic mechanisms by the presence of water molecules or side chains in the vicinity of asparte [Ac(−) in our complexes] (see, for instance, Ref. 43).

B. Geometries

The comparison of structural data before and after the H transfer shows that the changes of intermolecular parameters in Im-Ac(−) are greater than in Im(+)-Ac(−).[58] The relative orientation of imidazole and carboxylate planes is found to have a tendency towards coplanarity upon the H transfer in Im-Ac(−) while it changes very little in Im(+)-Ac(−). On the other side, since N···O distances are fixed, local geometry around the hydrogen bond remains nearly unchanged along the proton transfer so that only small deviations, less than 10° from linearity, are found in both complexes.[58] However, much more interesting for exploring the role played by the atoms involved in the interaction is the information supplied by internal geometry changes occurring in imidazole and carboxylate. This is displayed in Fig. 2 where the five bond lengths of the imidazole ring and the two ones of carboxylate at all the optimized geometries along the proton transfer are plotted including their corresponding monomer values. Note how the different CN lengths parallel the conventional picture given by the usual resonance forms: N_7C_9 and C_3N_1 bond lengths are larger and remain nearly constant upon the H transfer in both complexes whereas the shorter N_1C_5 and C_5N_7 bonds suffer opposite changes in Im-Ac(−) and Im(+)-Ac(−). In isolated neutral imidazole with H_1 bonded to N_1 these two bonds have different lengths that agree with the $N_7{=}C_5$ and C_5-N_1 image. When the ring interacts with acetate and H_1 is being transferred, both lengths converge in Im-Ac(−) toward a common value in the anionic Im(−) left behind after the H-transfer completion. In the limit of isolated Im(−) monomer this common length ~1.36 Å suggests that the negative charge is delocalized between two identical bonds in the $N_7C_5N_1$ moiety which has no H bonded to N. On the contrary, the imidazole ring in Im(+)-Ac(−) starts with equal C_5N_7 and N_1C_5 bond lengths ~1.34 Å which again suggests delocalization of positive charge in Im(+), as the resonance form depicted in the bottom panel of Fig. 2 indicates. When this ring interacts with acetate and H_1 is

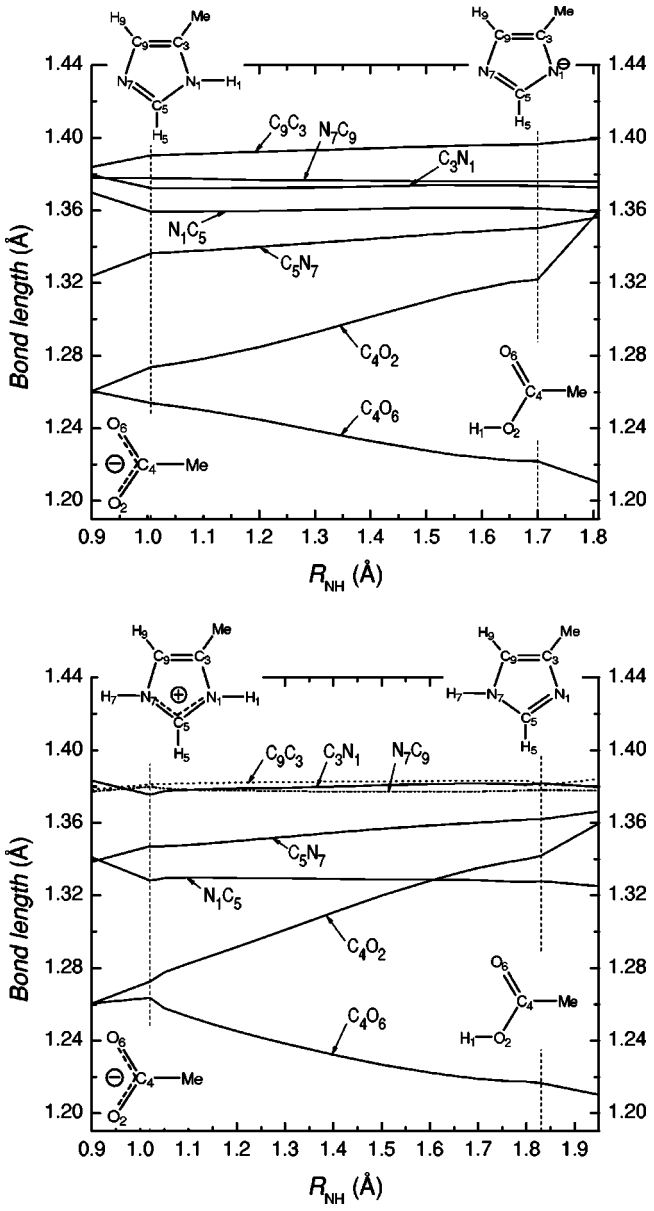

FIG. 2. Change upon proton transfer of internal bond lengths of imidazole ring and carboxylate in Im-Ac(−) (top panel) and Im(+)-Ac(−) (bottom panel). Proton transfer occurs at R_{NH} distances inside vertical dashed lines. Bond lengths converge to values for the corresponding monomers indicated by structural formulas at both ends of the process.

being transferred, that common length splits into two values, suggesting now the N_7-C_5 and $C_5{=}N_1$ image; i.e., the single/double pattern is inverted with respect to Im-Ac(−) because H is now bonded to N_7 instead to N_1, although the length of the $N_7{=}C_5$ and $C_5{=}N_1$ double bonds in both isomers of neutral imidazole is identical and the same happens in C_5-N_1 and N_7-C_5 single bonds. Note also how the C_9C_3 bond is slightly longer in Im-Ac(−) than in Im(+)-Ac(−), though virtually no change is noticed not only along proton transfer but also among the four isolated monomers.

If imidazole starts and ends at different forms giving rise to four distinct structures (drawn in Fig. 2), acetate suffers exactly the same change in the two complexes accepting H to become acetic acid. In fact, isolated monomer acetate shows two identical CO bond lengths (1.260 Å) that agree

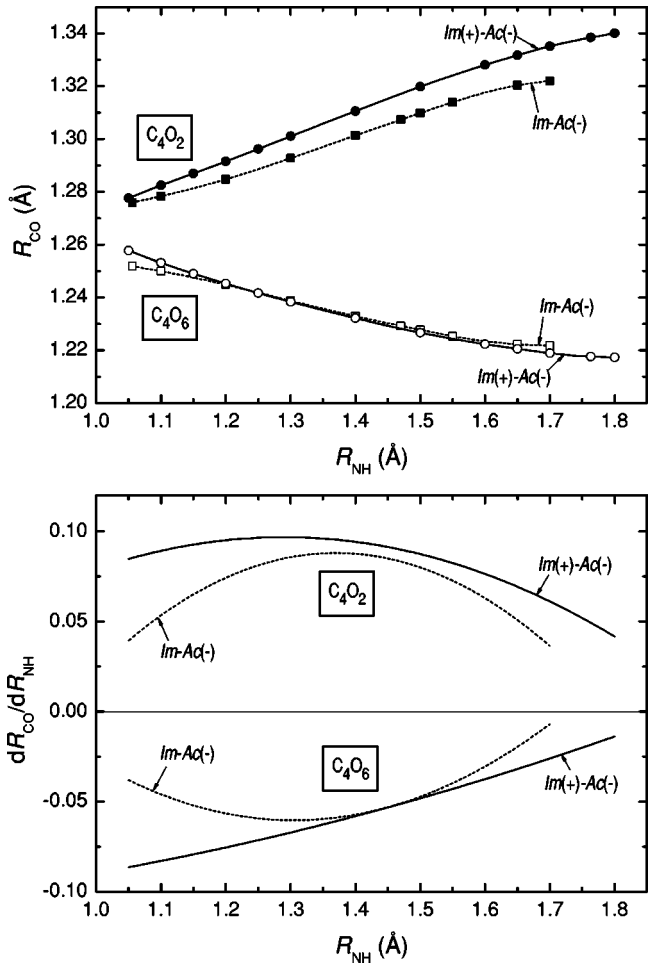

FIG. 3. Change upon proton transfer of internal bond lengths of carboxylate (R_{CO}) in Im-Ac(−) and Im(+)–Ac(−) (top panel) and derivative of R_{CO} with respect to R_{NH} (bottom panel).

with the conventional resonance form of carboxylate, whereas isolated monomer acetic acid shows one shorter C=O bond length (1.210 Å) and one longer C–OH bond length (1.360 Å) in agreement with the carboxylic structure. Therefore, when both monomers interact in the complexes and the H transfer progresses, converting acetate into acetic acid, the C_4O_2 bond elongates whereas C_4O_6 shortens. Moreover, since acetate lacks the severe geometrical constraints of rings, CO lengths are able to vary in much greater intervals and represent thus more sensitive probes to analyze geometry changes. Some interesting differences between complexes arise, as noticed in Fig. 3 where we have plotted separately this variation for ease of comparison. While the decrease of the C_4O_6 length from carboxylate toward carbonyl values is very similar in both systems, the increase of C_4O_2 is greater in Im(+)-Ac(−) than in Im-Ac(−) at all the stages of the H transfer. Since O_2 is directly involved in the interaction and increased C_4O_2 lengths are associated to the N_1-$H_1\cdots O_2 \rightarrow N_1\cdots H_1$-$O_2$ transformation in these curves, the fact that one of the complexes had, at a given R_{NH} a C_4O_2 length longer than the other can be interpreted in terms of greater affinity for H_1. Hence, the greater bond lengths in Im(+)-Ac(−) should mean that acetate is a better H acceptor from the H donor cationic imidazolium than from the H donor neutral imidazole which, in turn, agrees with the results displayed in Fig. 1 where the energy profiles show that proton transfer is more favored in Im(+)-Ac(−) than in Im-Ac(−).

The smooth behavior shown by all the curves in Fig. 2 indicates that the structural changes associated with electron distribution rearrangements occurring throughout the H transfer do not reveal any sudden change that could identify covalent bond breaking and hydrogen-bond formation in the N_1-$H_1\cdots O_2 \rightarrow N_1\cdots H_1$-$O_2$ transformation. However, given the greater sensitivity of CO lengths remarked above, their rate of change happens to provide a slight distinctive feature as it is readily seen in the bottom panel of Fig. 3 where we have plotted the derivatives of these lengths with respect to R_{NH}. The positive derivative of increasing C_4O_2 lengths shows a region of maxima at intermediate distances in both complexes [for Im-Ac(−) the maximum is at $R_{NH}=1.37$ Å and for Im(+)-Ac(−) at 1.29 Å], i.e., the increasing rate changes from convex to concave. A similar behavior is found for the decreasing C_4O_6 length only in Im-Ac(−) whose negative derivative is minimum at $R_{NH}=1.31$ Å, whereas it decreases uniformly in Im(+)-Ac(−). Although this result is, of course, too subtle to elaborate on, the fact that the most sensitive bond length taking no *direct* part into hydrogen bonding shows an inflection point at intermediate R_{NH} distances will be considered below in the discussion of other features associated to the N···H···O situation.

C. Natural population analysis charges

The natural bond orbital (NBO) procedure analyzes molecular wave functions in terms of one-center (lone pair) and two-center (bond) localized electron-pair units. Electron populations obtained from natural orbitals allow thus the exploration of electronic changes in traditional chemical (Lewis) terms of lone pairs and bonds. Besides this useful feature, NPA charges are known to be one of the most reliable population schemes that make use of the basis functions.[59] The information provided by NBO analyses should be especially valuable in the study of electron localization changes occurring upon hydrogen bonding, as it was pointed out by Weinhold some years ago.[4] We plot in Figs. 4 and 5 changes of NBO populations computed at all the optimized geometries for Im-Ac(−) and Im(+)-Ac(−), respectively. Imidazole values in Im-Ac(−) show double-bond populations about 4.2 *e* for C_5N_7 and C_3C_9 and 2.0 *e* for N_1C_5, N_1C_3, and N_7C_9 single bonds and one lone pair at N_7, in consistency with the bonding picture given by resonance forms. Single-bond and N_7 lone-pair populations remain constant upon proton transfer while double-bond populations increase very little, showing a smooth transition between monomers. Note, however, the evolution of N_1—from a lone-pair population of 1.64 *e* in isolated Im monomer, it decreases to 1.56 *e* at the first point in the complex and to 1.51 *e* at $R_{NH}=1.3$ Å and then suddenly rises to 3.25 *e* at 1.4 Å, remaining nearly unchanged until the completion of the H transfer with a population which is essentially that of the isolated Im(−) monomer (3.31 *e*). The data for carboxylate show double-bond values for C_4O_6 decreasing from 4.31 *e* in

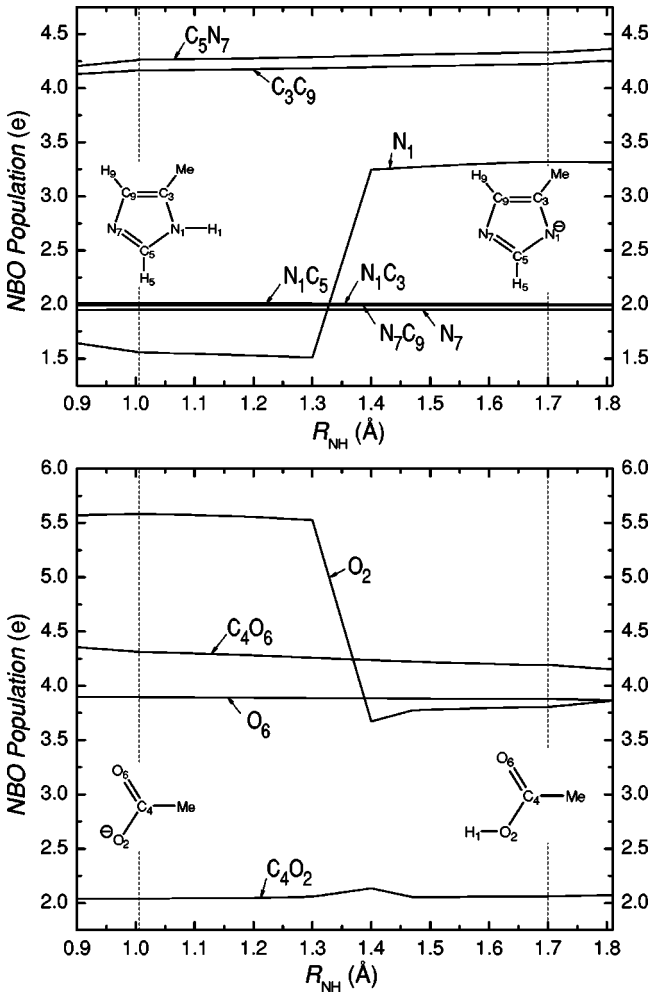

FIG. 4. Change upon proton transfer of NBO electron populations for imidazole (top panel) and carboxylate (bottom panel) in Im-Ac(−). Proton transfer occurs at R_{NH} inside vertical dashed lines. NBO populations converge to values for the localized forms indicated by resonance formulas of the corresponding monomers at both ends of the process.

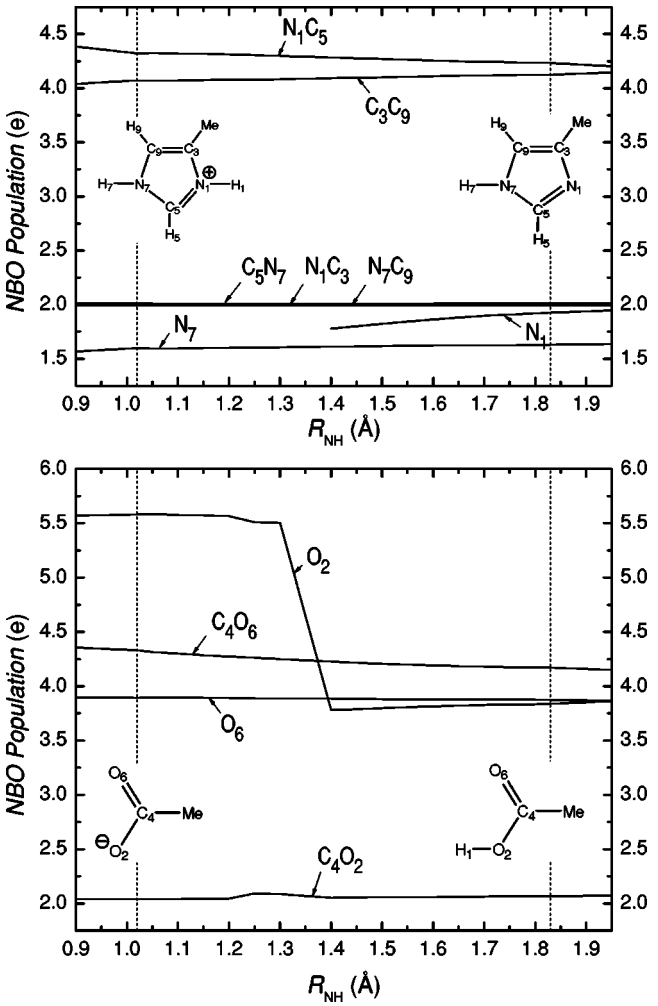

FIG. 5. Same as Fig. 4 for Im(+)-Ac(−).

acetate to 4.19 *e* in acetic acid and a nearly constant population of 3.9 *e* for O_6 which reveals the consistent presence of two lone pairs in this oxygen, irrespective of proton transfer. The C_4O_2 bond shows a constant single-bond value of 2.04 *e* except at $R_{NH}=1.4$ Å where it rises to 2.14 *e*. The lone-pair evolution of O_2 is again the distinctive feature, remaining about 5.5 *e* in isolated Ac(−) and in the complex until $R_{NH}=1.3$ Å to fall then suddenly to 3.67 *e* at 1.4 Å and 3.81 *e* upon the H-transfer completion and to 3.86 *e* in isolated acetic acid. These data are consistent with the bonding image given by the resonance form of acetate that has a C_4O_6 double bond and a negative charge at O_2 Figure 5 shows these changes for Im(+)-Ac(−). The imidazole data display double-bond populations for N_1C_5 and C_3C_9, changing very little from isolated monomers throughout, the H transfer, while C_5N_7, N_1C_3, and N_7C_9 exhibit single-bond constant values about 2.0 *e*, and N_7 shows one lone-pair population about 1.6 *e* in consistency with the bonding image of the resonance form of imidazolium cation. The evolution of N_1 is again the distinctive feature—its lone-pair population appears only at $R_{NH}=1.4$ Å with a value of 1.78 *e* rising then steadily to 1.95 *e* after the proton transfer completion. The population data for the carboxylate show nearly identical behavior to Im-Ac(−) except for the minor difference of the tiny maximum of C_4O_2 which is now at 1.25 Å instead of 1.4 Å, as noticed in Fig. 4.

The localization scheme performed by NBO analyses gives rise to assignment of electron pairs that give a bonding picture at variance with the unlocalized image inherent in geometry analyses discussed in the preceding paragraph. The interest in NBO information determined along the proton transfer is its ability to identify the particular stage at which a breaking point clearly appears in the interaction, which is not possible to do neither with geometry nor with electron-density data discussed below. In fact, the sudden changes in lone-pair populations of N_1 and O_2 noticed in Figs. 4 and 5 between $R_{NH}=1.3$ and 1.4 Å indicate that neat charge transfer occurs just at this region. In Im-Ac(−) a loss of 1.86 *e* in O_2 is accompanied by gains of 1.74 *e* in N_1 and 0.08 *e* in C_4O_2 bond, while in Im(+)-Ac(−) the loss of charge in O_2, 1.72 *e*, is nearly equal to the gain in N_1, 1.77 *e*. Hence, the distinctive feature revealed by the NBO data when a hydrogen bond forms is the changes suffered by the lone-pair populations of atoms bonded to H, changes that can be rationalized in terms of "charge transfer" which, as suggested by Weinhold,[4] should thus be a key element of analysis to investigate hydrogen bonding. To end this discussion, see

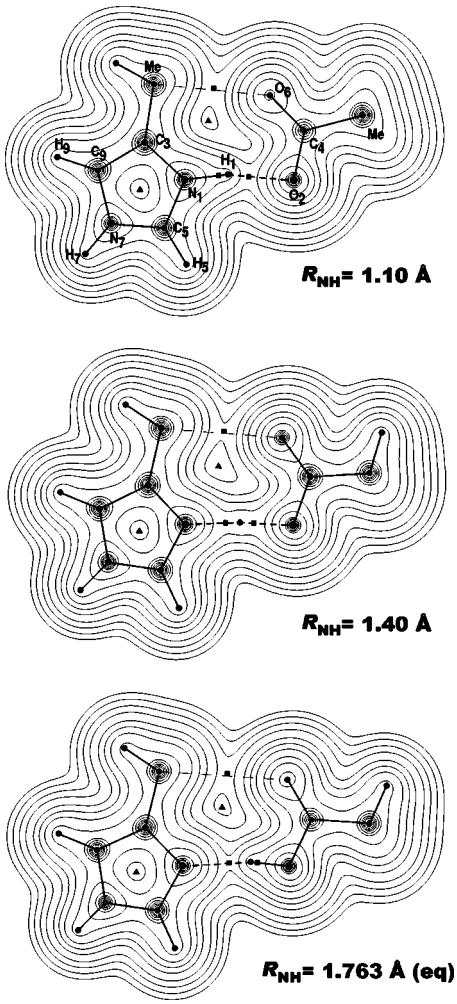

FIG. 6. MP2/6−311++G(d,p) electron density contour maps at the plane containing imidazole and carboxylate in Im(+)-Ac(−) at three H-transfer stages corresponding to the R_{NH} distances given. The outermost contour is $\rho(\mathbf{r})=0.001$ au while the rest of the contours are 2×10^n, 4×10^n, and 8×10^n au with $n=-3,-2,-1$, 0, 1, and 2. Small circles indicate nuclear positions, squares denote BCPs (only the two ones around H_1 and that at the bond path between methyl of imidazole and O_6 atom are drawn), and squares denote RCPs.

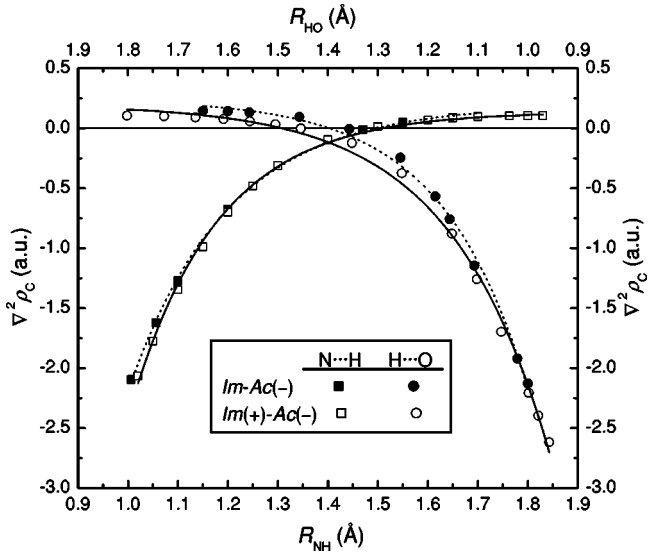

FIG. 7. Change upon H_1 transfer of local values of the Laplacian of $\rho(\mathbf{r})$ at the two BCPs around H_1, $\nabla^2\rho_C$, for Im-Ac(−) and Im(+)-Ac(−). Left Y axis and bottom X axis plot $\nabla^2\rho_C$ for N_1H_1 bond against its bond length R_{NH}, while right Y axis and top X axis plot $\nabla^2\rho_C$ for H_1O_2 bond against its bond length R_{HO}. Lines connecting points are exponential fits (see the text), dashed for Im-Ac(−) and solid for Im(+)-Ac(−).

how C_4O_2 bond happens to sense residually that charge transfer, especially in Im-Ac(−). It is worth recalling that, as remarked in the preceding paragraph and illustrated in Fig. 3, the increasing lengthening of this bond shows an inflection point just at the R_{NH}=1.3-1.4 Å interval more markedly for Im-Ac(−).

D. Electron densities

Before addressing the information supplied by topological descriptors of $\rho(\mathbf{r})$, it is worth remarking a feature of the electron density itself which is usually not highlighted enough, namely, its great numerical value around partners linked by hydrogen bonds. Figure 6 plots isocontour maps of $\rho(\mathbf{r})$ for Im(+)-Ac(−) at three geometries corresponding to stages N_1-$H_1\cdots O_2$(R_{NH}=1.10 Å), $N_1\cdots H_1\cdots O_2$(1.40 Å), and $N_1\cdots H_1$-O_2 (1.763 Å, minimum in Fig. 1). As for the contours plotted starting at the outermost one, the last isocontour that embraces imidazole and carboxylate moieties around the $N_1H_1O_2$ bond path is $\rho(\mathbf{r})=0.08$ a.u. in the middle map and 0.04 a.u. in the other two maps. If one recalls that 0.001 or 0.002 a.u. are values usually chosen to estimate molecular van der Waals volume[33] as well as to set molecular shape,[60] isocontours as great as 0.04–0.08 a.u. are indicative of space regions with considerably large electron density, which is indeed an evidence in favor of a quantum electron image against a classical electrostatic one to be taken into account when discussing the ultimate nature of hydrogen bonding.

Figure 6 also shows bond critical points (BCPs) as well as ring critical points (RCPs) of the electron density. The AIM topological analysis predicts in most geometries a second intermolecular BCP in the bond path formed by C and one H atom (actually outside the plane of these plots) in methyl of imidazole and O_6 atom of carboxylate (this path is drawn as a line with large dashes in Fig. 6). As a consequence, the system has a second RCP besides that of imidazole ring. However, since we are here interested in the interaction underlying the H_1 transfer and the properties of this second C–H···O hydrogen bond remain unchanged at all the geometries, we shall ignore it in the rest of the paper focusing on descriptors relevant to the main $N_1H_1O_2$ bond path. Hence, we select the two BCPs around H_1 as probes to explore the transformation N_1-$H_1\cdots O_2\rightarrow N_1\cdots H_1\cdots O_2\rightarrow N_1\cdots H_1$-$O_2$ by plotting together the changes with distance between N_1 and H_1(R_{NH}) and between H_1 and O_2(R_{HO}) of local values of the following properties at these BCPs: electron density, ρc,[61] Laplacian of the electron density, $\nabla^2\rho$c (Fig. 7), and total energy density, Hc (Fig. 8). Three-parameter exponential fits of the type $Y=Y_0+\alpha^*\mathrm{Exp}(-b^*x)$ are also drawn for every descriptor Y, being $x=R_{NH}$ or R_{HO}. The goodness of this representation is illustrated by the R^2 values found between 0.99996 and 1.0 for ρc, between 0.9969 and 0.9994 for $\nabla^2\rho$c, and between 0.9981 and 0.9998 for Hc. Since the domain of distances covers the covalent →

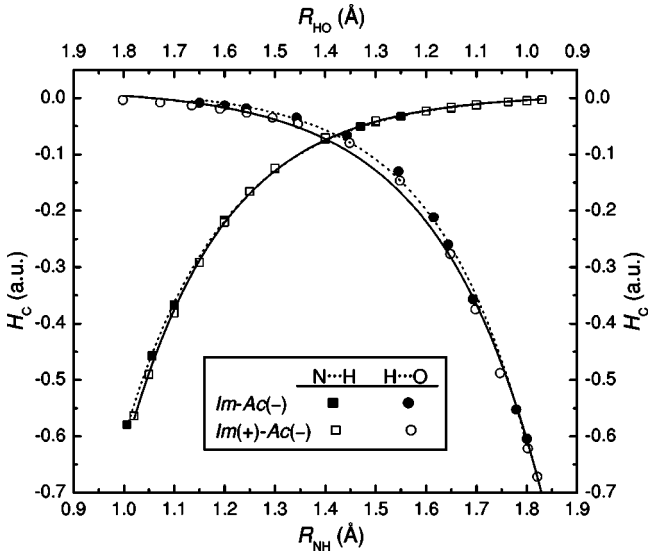

FIG. 8. Change upon H transfer of local values of the total-energy density at the two BCPs around H_1, H_C, for Im-Ac(−) and Im(+)-Ac(−). Left *Y* axis and bottom *X* axis plot H_C for N_1H_1 bond against its bond length R_{NH}, while right *Y* axis and top *X* axis plot H_C for H_1O_2 bond against its bond length R_{HO}. Lines connecting points are exponential fits (see the text), dashed for Im-Ac(−) and solid for Im(+)-Ac(−).

hydrogen bond transit, this result reveals that the properties obtained from $\rho(\mathbf{r})$ vary continuously and smoothly along that transformation without showing any sort of breaking characteristics that could identify neat boundaries.

The exponential behavior of topological descriptors with the intermolecular distance in hydrogen-bond systems has been repeatedly reported before (see, for instance, the reviews by Grabowski[24] and Steiner[25] or the paper by Espinosa and Molins,[62] and references therein). However, this behavior has been referred to *distinct* systems with different hydrogen-bond lengths either theoretically computed or experimentally observed. We have also reported[6,32,46] similar studies for wider ranges of distances (covering lengths inside equilibrium) *within the same* complex, but the behavior of descriptors of $\rho(\mathbf{r})$ at the transit between covalent and hydrogen bonds has deserved much less attention. In this regard, the single exception (as far as we are aware) is the recent work of Espinosa *et al.*[8] where some descriptors were studied on X–H···F–Y systems and isolated pairwise H···F interactions at a large set of distances covering covalent and hydrogen-bond regimes. Although the authors also found a continuous behavior at domains associated to changes from weak to strong interaction, the presence of many geometries at the long range in their data gave rise to different exponential functionalities at long and short lengths which led them to propose a joint function permitting fitted representations throughout the full range of distances. On the contrary, insofar as our work here involves definite range limits associated to the proton transfer studied, our analysis regards just the covalent → hydrogen bond transit.

The evidence gathered after years of AIM studies on intermolecular interactions led to the proposal of eight criteria based solely on information obtained directly from $\rho(\mathbf{r})$ to characterize hydrogen bonding.[34,63] Two of these criteria concern the magnitude of ρc and $\nabla^2\rho$c. According to them a hydrogen-bond path must have a $(3,-1)$ BCP with values within the range 0.002–0.04 a.u. for the electron density and 0.02–0.15 a.u. for its Laplacian.[34,63] Greater values of $\rho(\mathbf{r})$ at interatomic regions mean usually stronger local bonding due to the known exponential decaying behavior of the electron density at long distances. Therefore, stronger hydrogen bonds are expected to show greater values of ρc as it has been before demonstrated in a variety of complexes.[24,25] Regarding our complexes, the smallest values of ρc are already near the upper limit set by the first criterion,[61] which indeed suggests that these are very strong hydrogen bonds. Except for minor details due to their different intermolecular separations, the two complexes show similar behaviors, displaying ρc about 0.31–0.35 a.u. in N_1-H_1 and H_1-O_2 covalent bonds and 0.038–0.054 a.u. in $H_1\cdots O_2$ and $N_1\cdots H_1$ hydrogen bonds at both the extreme stages of H transfer. The curves cross at $R_{NH}=1.43$ Å in Im-Ac(−) and 1.41 Å in Im(+)-Ac(−) at the $N_1\cdots H_1\cdots O_2$ middle stage where both bond paths around H_1 show $\rho c\sim 0.11$ au a value nearly three times the upper limit of the AIM criterion which indicates rather strong hydrogen bonding at that region.[61] As for the Laplacian of $\rho(\mathbf{r})$, Fig. 7 shows a nearly undistinguishable behavior for N···H paths with $\nabla^2\rho c$ entering the positive domain at $R_{NH}\sim 1.50$ Å in both complexes, while for H···O paths $\nabla^2\rho c>0$ at $R_{HO}=1.35$ Å in Im-Ac(−) and 1.45 Å in Im(+)-Ac(−) (this 0.1-Å difference is just the difference in the intermolecular N···O distances of both complexes). Recall that in the AIM theory, strong shared-shell interatomic interactions are characterized by local concentration of charge ($\nabla^2\rho(\mathbf{r})<0$), whereas weak closed-shell interactions exhibit local depletion of charge ($\nabla^2\rho(\mathbf{r})>0$). Therefore, interatomic paths can be classified as shared shell (covalent) if $\nabla^2\rho c<0$ or closed shell (hydrogen bond) if $\nabla^2\rho c>0$ and $\nabla^2\rho c=0$ sets then the boundary between both types of interaction which in our complexes occurs at $R_{NH}=1.5$ Å corresponding to the middle N···H···O stage. However, all the $\nabla^2\rho c>0$ values are very small, which suggests that the underlying interactions are not characterized by strong depletion of charge, i.e., they remain as strong hydrogen bonds.

The total energy density at $\mathbf{r}=\mathbf{x}$, $H(\mathbf{x})$, is the sum of the kinetic energy density $G(\mathbf{x})$ and the potential energy density $V(\mathbf{x})$ at that point. Since $G(\mathbf{x})$ is always positive and $V(\mathbf{x})$ always negative, the sign of $H(\mathbf{x})$ indicates what is the dominant contribution at $\mathbf{x}$ which is, in turn, related with the sign of $\nabla^2\rho(\mathbf{x})$.[33,34] Covalent bonds are characterized by large negative values of $H(\mathbf{r})$ at the BCP, Hc, whereas hydrogen bonds usually display small positive values of Hc. The presence of Hc<0 in a hydrogen-bond path is interpreted as a proof of strong interaction, and hence the hydrogen bond is assumed to have some degree of covalent character.[14,32,34,44] Figure 8 shows a smooth covalent → hydrogen bond transit for both complexes without never entering the Hc>0 domain. This suggests a persistence of a covalent character consistent with the strong nature of these hydrogen bonds.

A common feature revealed by the topological descriptors of $\rho(\mathbf{r})$ at both paths around the H being transferred is that they display essentially the same magnitude at the $R_{NH}=R_{HO}\sim 1.4$-Å region in their smooth evolution from covalent to hydrogen bonds. It should be stressed that, except for

the boundary set by $\nabla^2\rho c=0$, the covalent → hydrogen bond transit for the underlying interactions occurs without showing neither breaking points nor noticeable changes of trends which in turn indicates that this evolution associated to the proton transfer is accompanied by a continuous rearrangement of electron distribution in the systems.

E. Electron localization function

The ELF was defined by Becke and Edgecombe[38] as the Lorentzian-type expression $\eta(\mathbf{r})=1/(1+q^2)$, where $q=(T-T_w)/T_{\mathrm{TF}}$. In this quotient, T is the kinetic energy computed with the molecular orbitals, and T_w and T_{TF} are the von Weizsäcker and Thomas–Fermi kinetic energy functionals, respectively.[64] Whereas T_{TF} gives the kinetic energy of an electron gas with homogeneous density, T_w, computed as (except a numerical factor) $[\nabla\rho(\mathbf{r})]^2/\rho(\mathbf{r})$, accounts for inhomogeneity corrections.[64] From a physical point of view, $\eta(\mathbf{r})$ can be interpreted in terms of local excess kinetic-energy density $(T-T_w)$ due to the Pauli repulsion, giving thus a measure of the local electron localization in a system.[65] Because of its definition, the domain of the ELF is $0\leqslant\eta(\mathbf{r})\leqslant 1$. At regions where there is either an opposite spin electron pair or a single electron, the Pauli repulsion has little effect and $(T-T_w)\sim 0$, i.e., $T\approx T_w$ so that $\eta(\mathbf{r})\to 1$. At regions where the probability of finding electrons with parallel spins is high, $(T-T_w)$ is large and $\eta(\mathbf{r})\to 0$. The middle value $\eta(\mathbf{r})=1/2$ means $T=T_w\pm T_{\mathrm{TF}}$ which represents a homogeneous electron-gas pair probability,[65] i.e., electron delocalization.

Figure 9 plots isocontour maps of the ELF at the plane containing imidazole and carboxylate groups in Im(+)-Ac(−) (maps for Im-Ac(−) are rather similar). While the outermost $\eta(\mathbf{r})=0.01$ isocontour surrounds the whole complex, tracing out its bulk volume, the immediately following contours embrace the partners, tracing out separate profiles for methylimidazole and acetate. The set of $\eta(\mathbf{r})\geqslant 0.5$ isocontours define localization domains which split the system into distinct groups. Focusing upon the proton transfer region, see how N_1–H_1 and O_2 domains initially separated at the 1.10-Å stage merge into a $N_1\cdots H_1\cdots O_2$ common domain at 1.40 Å and finally split again into N_1 and H_1–O_2 domains after the proton transfer completion at 1.763 Å. It is interesting to compare the shape of domains defined by the boundary contour $\eta(\mathbf{r})=1/2$ in these maps. At the initial stage they shrink around the H_1 atom in the N_1–H_1 bond and around the lone-electron pair in O_2 oriented toward H_1. Compare these shapes with those of N_7–H_7 bond in imidazole and O_4 in carboxylate, respectively. At the final stage, these domains show similar deformation, shrinking now around H_1 in the H_1–O_2 bond and around the lone-electron pair in N_1 oriented toward H_1. This feature, observed before in hydrogen-bond systems at equilibrium geometries,[32,66] reveals a tight spatial electron localization associated to the covalent bond of the H-donor group and the lone pair of the H-acceptor atom. However, at the intermediate $N_1\cdots H_1\cdots O_2$ situation where hydrogen is approximately equally shared by the donor and acceptor atoms, the localization domain changes, extending over the three atoms, but concentrates on hydrogen itself as it is illustrated by the accumulation of contours with high $\eta(\mathbf{r})$ values around H_1 in the middle map of Fig. 9. These changes in the ELF suggest that hydrogen bonding is accompanied by strong electron localization at intermolecular regions where the interaction is linking the partners, reaching a maximum effect just at equal sharing arrangements like $N_1\cdots H_1\cdots O_2$. From the point of view that we emphasize in this work, namely, the nature of the interaction underlying hydrogen bonding, these results call again for the need of full quantum methods instead of classical electrostatic approaches to treat hydrogen-bond systems.

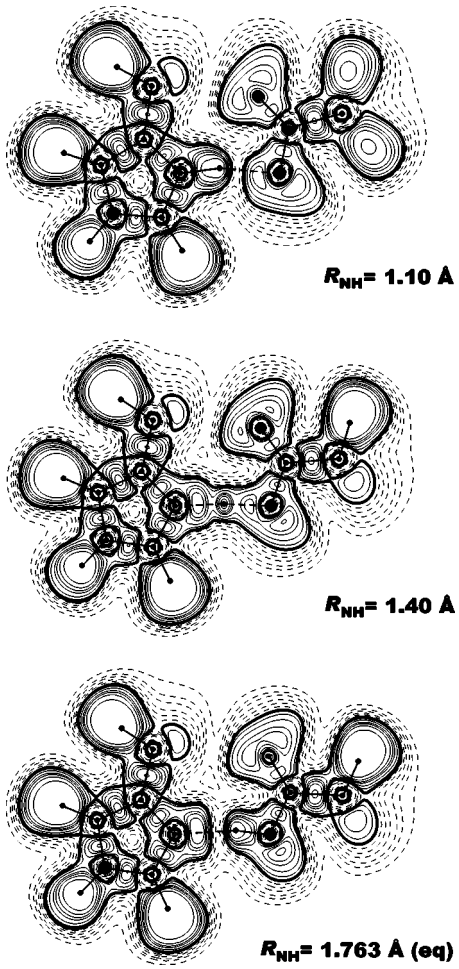

FIG. 9. Electron localization function $\eta(\mathbf{r})$ contour maps for Im(+)-Ac(−). Structures and relative orientations as in Fig. 6. From the outermost isocontour, dashed lines give increasing $\eta(\mathbf{r})=0.01$, 0.05, 0.1, 0.2, 0.3, and 0.4. The thicker line gives then the $\eta(\mathbf{r})=0.5$ isocontour, and solid lines correspond to increasing 0.6, 0.7, 0.8, 0.9, and 0.95 isocontours.

IV. CONCLUSIONS

We have studied the proton transfer from 4-methylimidazole unprotonated, Im, and protonated, *Im*(+), to acetate, *Ac*(−), by means of MP2/6-311++G(*d*,*p*) *ab initio* calculations. These complexes model diads formed by side chains of histidine (neutral and protonated) and aspartate, and the H transfer represents their interaction in enzymes at distinct stages of many catalytic mechanisms. Our main goal in exploring this process is to gain insight into the

nature of the interaction underlying associated hydrogen bonds.

Our calculations predict in Im-Ac(−) a minimum for H bonded to Im and a near barrierless process for the H transfer to Ac(−), resulting in an energy 6 kcal/mol higher. On the contrary, protonating imidazole in Im(+)-Ac(−) favors the H transfer in a downhill process that leads to an energy 20 kcal/mol lower for the H transferred to acetate to yield acetic acid.

While the structures remain nearly unaltered, the small variation of bond lengths in imidazole and carboxylate allows the tracking of the subtle electron rearrangements associated to the process $N–H\cdots O \rightarrow N\cdots H\cdots O \rightarrow N\cdots H–O$. These changes connect the geometries of complexes at initial and final stages of the H transfer with those of the corresponding isolated monomers at structures that show in all cases the bond pattern suggested by the most important resonance forms. However, the evolution of these parameters fails to exhibit discontinuities that could reveal a formation or breaking of hydrogen bonds.

The NBO populations for bonds and lone pairs confirm the single-/double-bond pattern suggested by geometry parameters. However, contrary to the rest of properties analyzed, there appears a discontinuity that clearly reveals a breaking point in the proton transfer, that is, when H has moved 1.3 Å from imidazole the population of electron lone pairs in N and O happens to suffer a sudden change associated to the switching $N–H\cdots O \rightarrow N\cdots H–O$.

Neither the spatial distribution of electron density nor the variation of its topological descriptors shows any type of discontinuity along the transit covalent → hydrogen bonding involved in the process. On the contrary, the smooth evolution of features computed at both bonds around the H atom being transferred from covalent to hydrogen bonding along the whole transfer is well reproduced by means of single exponential fits. The magnitude of the descriptors studied is consistent with the existence of very strong hydrogen bonds.

The changes suffered by the distribution of the ELF suggest that hydrogen bonding is accompanied by strong electron localization at intermolecular regions. This reaches a maximum effect at the middle stage $N\cdots H\cdots O$ for which a continuous localization domain showing large values of the ELF is shared by chemical groups linked by hydrogen bonds.

All these conclusions can be summarized in a single one: The evolution from covalent to hydrogen bonding is a continuous process characterized by a smooth rearrangement of the electron distribution and concomitantly smooth structural changes. Regarding our attempt to address the nature of hydrogen bonding, this work suggests that the underlying interaction must be described in terms of electron redistribution in the intermolecular space much like the covalent bonding. It seems evident that only studies using full quantum approaches are capable of accounting for the characteristics of an interaction that is currently far from the simple electrostatic image managed until a few years ago.

ACKNOWLEDGMENT

The authors gratefully acknowledge the Direccion General de Investigacion del Ministerio de Ciencia y Tecnologia for financial support, Project No. BQU2002-04005.

[1] G. N. Lewis, *Valence and the Structure of Atoms and Molecules* (Chemical Catalog, New York, 1923).
[2] L. Pauling, *The Nature of Chemical Bond*, 2nd ed. (Cornell University Press, Ithaca, NY, 1940).
[3] F. Hibbert and J. Emsley, Adv. Phys. Org. Chem. **26**, 255 (1990).
[4] F. Weinhold, J. Mol. Struct.: THEOCHEM **399**, 181 (1997).
[5] T. K. Ghanty, V. N. Staroverov, P. R. Koren, and E. R. Davidson, J. Am. Chem. Soc. **122**, 1210 (2000).
[6] O. Gálvez, P. C. Gómez, and L. F. Pacios, J. Chem. Phys. **115**, 11166 (2001).
[7] A. van der Vaart and K. M. Merz, J. Chem. Phys. **116**, 7380 (2002).
[8] E. Espinosa, I. Alkorta, J. Elguero, and E. Molins, J. Chem. Phys. **117**, 5529 (2002).
[9] T. K. Ghanty and S. K. Ghosh, J. Phys. Chem. A **107**, 7062 (2003).
[10] A. Ranganathan, G. U. Kulkarni, and C. N. R. Rao, J. Phys. Chem. A **107**, 6073 (2003).
[11] G. A. Kumar and M. A. McAllister, J. Org. Chem. **63**, 6968 (1998).
[12] F. Cordier and S. Grzesiek, J. Am. Chem. Soc. **121**, 1601 (1999).
[13] G. Cornilescu, J. S. Hu, and A. Bax, J. Am. Chem. Soc. **121**, 2949 (1999).
[14] W. D. Arnold and E. Oldfield, J. Am. Chem. Soc. **122**, 12835 (2000).
[15] W. H. Thompson and J. T. Hynes, J. Am. Chem. Soc. **122**, 6278 (2000).
[16] W. Qian and S. Krimm, J. Phys. Chem. A **106**, 6628 (2002).
[17] A. J. Barnes, J. Mol. Struct. **704**, 3 (2004).
[18] E. D. Isaacs, A. Shukla, P. M. Platzman, D. R. Hamann, B. Barbiellini, and C. Tulk, Phys. Rev. Lett. **82**, 600 (1999).
[19] B. Barbiellini and A. Shukla, Phys. Rev. B **66**, 235101 (2002).
[20] B. King and F. Weinhold, J. Chem. Phys. **103**, 333 (1995).
[21] S. Jenkins and I. Morrison, Chem. Phys. Lett. **317**, 97 (2000).
[22] T. Kortemme, A. V. Morozov, and D. Baker, J. Mol. Biol. **326**, 1239 (2003).
[23] A. V. Morozov, T. Kortemme, K. Tsemekhan, and D. Baker, Proc. Natl. Acad. Sci. U.S.A. **101**, 6946 (2004).
[24] S. J. Grabowski, J. Phys. Org. Chem. **17**, 18 (2003).
[25] T. Steiner, Angew. Chem., Int. Ed. **41**, 48 (2002).
[26] J. Poater, X. Fradera, M. Sola, M. Duran, and S. Simon, Chem. Phys. Lett. **369**, 248 (2003).
[27] G. Desiraju and T. Steiner, *The Weak Hydrogen Bond in Structural Chemistry and Biology* (Oxford University Press, Oxford, UK, 1999).
[28] I. Alkorta, I. Rozas, and J. Elguero, Chem. Soc. Rev. **27**, 163 (1998).
[29] M. J. Calhorda, Chem. Commun. (Cambridge) **2000**, 801.
[30] C. L. Perrin and J. B. Nielson, Annu. Rev. Phys. Chem. **48**, 511 (1997).
[31] L. C. Remer and J. H. Jensen, J. Phys. Chem. A **104**, 9266 (2000).
[32] L. F. Pacios, J. Phys. Chem. A, **108**, 1177 (2004).
[33] R. F. W. Bader, *Atoms in Molecules: A Quantum Theory* (Clarendon, Oxford, UK, 1990).
[34] P. Popelier, *Atoms in Molecules: An Introduction* (Prentice-Hall, Harlow, UK, 2000).
[35] B. Silvi and A. Savin, Nature (London) **371**, 683 (1994)
[36] S. Nouri, F. Colonna, A. Savin, and B. Silvi, J. Mol. Struct. **450**, 59 (1998).
[37] F. Fuster, A. Savin, and B. Silvi, J. Phys. Chem. A **104**, 852 (2000).
[38] A. D. Becke and K. E. Edgecombe, J. Chem. Phys. **92**, 5397 (1990).
[39] W. W. Cleland and M. M. Kreevoy, Science **264**, 1887 (1994).
[40] W. W. Cleland, P. A. Frey, and J. A. Gerlt, J. Biol. Chem. **273**, 25529 (1998).
[41] W. W. Cleland, Arch. Biochem. Biophys. **382**, 1 (2000).
[42] W. M. Westler, F. Weinhold, and J. L. Markley, J. Am. Chem. Soc. **124**, 14373 (2002).
[43] P. A. Molina and J. H. Jensen, J. Phys. Chem. B **107**, 6226 (2003).
[44] L. F. Pacios and P. C. Gómez, J. Phys. Chem. A **108**, 11783 (2004).
[45] O. Gálvez, P. C. Gómez, and L. F. Pacios, Chem. Phys. Lett. **337**, 11166 (2001).
[46] O. Gálvez, P. C. Gómez, and L. F. Pacios, J. Chem. Phys. **118**, 4878 (2003).
[47] L. F. Pacios, Struct. Chem. (in press).
[48] A. E. Reed and F. Weinhold, J. Chem. Phys. **78**, 4066 (1983).
[49] A. E. Reed, R. B. Weinstock, and F. Weinhold, J. Chem. Phys. **83**, 735 (1985).

[50]A. E. Reed and F. Weinhold, J. Chem. Phys. **83**, 1736 (1985).
[51]A. D. Rabuck and G. E. Scuseria, Theor. Chem. Acc. **104**, 439 (2000).
[52]F. W. Biegler-Konig, R. F. W. Bader, and T. H. Tang, J. Comput. Chem. **3**, 317 (1982).
[53]E. D. Glendening, J. K. Badenhoop, A. E. Reed, J. E. Carpenter, and F. Weinhold, NBO 4.0, Theoretical Chemistry Institute, University of Wisconsin, Madison, WI, 1996.
[54]J. Kong, C. A. White, A. I. Krylov *et al.*, J. Comput. Chem. **21**, 1532 (2000).
[55]M. J. Frisch, G. W. Trucks, H. B. Schlegel *et al.*, GAUSSIAN 03, Gaussian, Inc., Wallingford, CT, 2003.
[56]L. F. Pacios, Comput. Biol. Chem. **27**, 197 (2003).
[57]P. C. Gómez and L. F. Pacios, Phys. Chem. Chem. Phys. **7**, 1374 (2005).
[58]See EPAPS Document No. E-JCPSA6-122-308521 for geometries of both complexes before and after the H transfer in Fig. 1. This document can be reached via a direct link in the online article's HTML reference section or via the EPAPS homepage (http://www.aip.org/pubservs/epaps.html).
[59]K. B. Wiberg and P. R. Rablen, J. Comput. Chem. **14**, 1504 (1993).
[60]P. Mezey, *Shape in Chemistry: An Introduction to Molecular Shape and Topology* (VCH, New York, 1993).
[61]For the plot of ρ_C against both distances around H_1 atom in Fig. 2, see Ref. 58.
[62]E. Espinosa and E. Molins, J. Chem. Phys. **113**, 5686 (2000).
[63]U. Koch and P. L. A. Popelier, J. Chem. Phys. **99**, 9747 (1995).
[64]R. G. Parr and W. Yang, *Density Functional Theory of Atoms and Molecules* (Oxford University Press, New York, 1989).
[65]A. Savin, O. Jepsen, J. Flad, O. K. Andersen, H. Preuss, and H. G. von Schnering, Angew. Chem., Int. Ed. Engl. **31**, 187 (1992).
[66]F. Fuster and B. Silvi, Theor. Chem. Acc. **104**, 13 (2000).